AIP | Journal of Applied Physics

Surface enhanced fluorescence and Raman scattering by gold nanoparticle dimers and trimers

Zhenglong Zhang, Pengfei Yang, Hongxing Xu, and Hairong Zheng

Citation: J. Appl. Phys. **113**, 033102 (2013); doi: 10.1063/1.4776227
View online: http://dx.doi.org/10.1063/1.4776227
View Table of Contents: http://jap.aip.org/resource/1/JAPIAU/v113/i3
Published by the American Institute of Physics.

JOURNAL OF APPLIED PHYSICS **113**, 033102 (2013)

Surface enhanced fluorescence and Raman scattering by gold nanoparticle dimers and trimers

Zhenglong Zhang,[1,2] Pengfei Yang,[2] Hongxing Xu,[2] and Hairong Zheng[1,a)]
[1]*School of Physics and Information Technology, Shaanxi Normal University, 710062 Xi'an, People's Republic of China*
[2]*Beijing National Laboratory for Condensed Matter Physics, Institute of Physics, Chinese Academy of Sciences, 100190 Beijing, People's Republic of China*

(Received 4 September 2012; accepted 28 December 2012; published online 16 January 2013)

Dimers and trimers of gold nanoparticles were synthesized using wet chemistry method for surface enhanced fluorescence and Raman scattering. The dimers and trimers provide hot spots for enhancing the fluorescence and Raman signals, and significantly obvious enhancement is obtained from Raman signals in solution. Using finite element method, we calculate the enhancement of fluorescence and Raman signals in the experimental system. Both experimental and theoretical results show that the dimers and trimers solution can be used in micro-quantitative detection from fluorescence and Raman signals. © *2013 American Institute of Physics*. [http://dx.doi.org/10.1063/1.4776227]

I. INTRODUCTION

To improve the fluorescence or Raman sensitivity and take the signals with a higher contrast, a powerful technique known as surface enhanced spectroscopy (SES)[1] has recently stimulated considerable interest in diverse applications of spectroscopy technology in non-destructive detection, biological and chemical sensing, and optical devices.[2–10] The localized enhanced near-field electromagnetic (EM) reported in the vicinity of metallic nanostructures can be mostly responsible for the SES effect such as surface enhanced fluorescence (SEF)[11,12] and surface enhanced Raman scattering (SERS).[13,14]

It is widely accepted that the SEF effect can arise from the two following origins:[12] an increase of the excitation magnitude due to the enhanced local EM and an increase of the emission magnitude due to the increased quantum yield of fluorescence (correlated to an increase of the radiative decay rate). Both of them should occur on a certain distance between molecule and metallic surface.[15,16] Due to the peculiar property of fluorescence, the interaction between the molecule and a metallic surface can lead to a quenching of the fluorescence, commonly observed when the distance between the molecule and the surface is less than a few nanometers. However, the relative contributions of SEF effect are still unclear and an enhanced fluorescence has been observed for molecules in direct contact with silver nanoparticles.[15]

Another powerful spectroscopy technique, know as SERS, has been suggested to be capable of single-molecule detection.[17,18] The very intense Raman enhancement observed in SERS is due to an EM enhancement from the metallic surface and a charge transfer mechanism between the adsorbed molecules and the metallic surface. The enhancement factor of SERS can be as much as 10^8 to 10^{12}, which is far more than SEF factor. In fact, a molecule situated on metallic surface thus experiences an excitation intensity that is enhanced by a factor $|E_{loc}(\omega)|^2/|E_{inc}(\omega)|^2$, where $E_{inc}(\omega)$ is the incident intensity of the EM fields with the optical frequency ω, and $E_{loc}(\omega)$ is the intensity of the local EM field. Also, the far field radiated by the molecule is enhanced by the factor $|E_{loc}(\omega')|^2/|E_{inc}(\omega')|^2$, where ω' now denotes the emission frequency, which is approximately equal to ω. It is clear that the overall Raman enhancement factor is proportional to $|E_{loc}(\omega)|^4/|E_{inc}(\omega)|^4$, that is only $|E_{loc}(\omega)|^2/|E_{inc}(\omega)|^2$ for fluorescence enhancement.[19]

It is established that the EM field enhancement in both SERS and SEF is due to the localized surface plasmon resonance (LSPR), a class of surface modes that involves the collective excitation of conduction electrons in response to the incident EM field.[20–23] For gold or silver nanoparticles (NPs), a drastically amplified EM field enhancement is presented in the nanogap between two NPs, which is called "hot spot" phenomenon.[24] In general, the dimeric structures are produced by using the biological or organic linkers, which prevent the analyte molecules enter into the nanogap, and the SES signals were interfered by the linker molecules.[25,26] Moreover, recent advances in SES have focused on a single dry dimer, which is produced by drying process. However, these methods lack collective behavior in solution, which is limited in SES applications.

In this paper, we use chemistry method to synthesize gold NPs (GNPs) dimers by introducing a small amount of sodium chloride into the reaction solution. It is found that not only dimers but also trimers can be obtained with reasonably high yields in one step. Then, the obvious SEF and SERS effects of Rhodamine 6G (Rh6G) were observed in solution by using gold dimers and trimers. The enhancement factors of dimers and trimers for SERS and SEF were calculated by finite element method (FEM), respectively. These findings offer a simple way of acquiring enhancement substrates in SES and its application to non-destructive detection in solution.

II. EXPERIMENTAL DETAILS

Uniform GNPs are fabricated by general reduction of chloroauric acid ($HAuCl_4$) by boiling with sodium citrate.

a)Electronic mail: hrzheng@snnu.edu.cn.

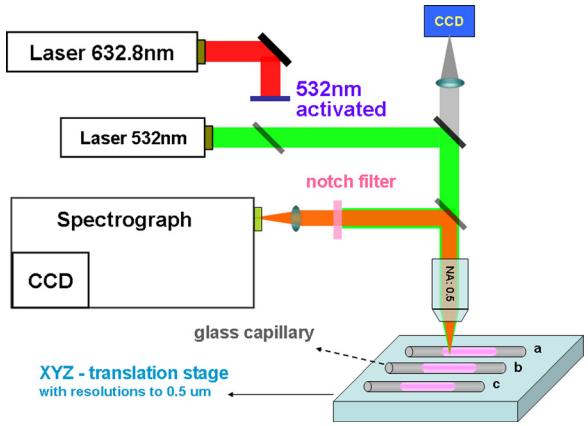

FIG. 1. The setup of the home-built confocal spectroscopic system.

First, in a round-bottomed flask equipped with a stirring bar, 2 ml of 1 wt. % $HAuCl_4$ and 40 ml deionized water were heated to boil with vigorous stirring. Second, 1 ml of 1 wt. % sodium citrate was added quickly, which resulted in a color change from blue to burgundy. After further stirring at the same temperature for 20 min, the resulting solution was cooled to room temperature. Third, we take half of the obtained solution out for further reaction, and then 50 μl of sodium chloride solution (NaCl, 5×10^{-3} M) was added to the other half of obtained solution and stirred for 20 min to modify the surface of the GNPs. Lastly, after the reactions had proceeded for 6 h, the two kinds of resulting GNPs were collected by centrifugation at 10 000 rpm for 5 min and washed twice with deionized water, respectively.

To investigate SEF and SERS from the GNPs solutions, 1 ml of the two solutions was added into 4 ml of Rh6G molecule solution (5×10^{-7} M) with 2 h reaction time, respectively. A small amount of the mixed solutions was transferred into the glass capillary for SEF and SERS experimental measurements. SEF and SERS spectra were measured with a home-built confocal spectroscopic system as shown in Figure 1. The samples were excited with 532 nm CW laser and 633 He-Ne laser with 50× objective. The appropriate notch filters were placed in front of the entrance of the SP2750i spectrometer (Acton Research Corporation, USA), and fluorescence and Raman spectra were detected using a PIXIS100 CCD detector (Acton Research Corporation, USA). The data acquisition time used in the experiment was 1 s for one spectrum.

III. RESULTS AND DISCUSSION

Figure 2 shows the typical scanning electron microscope (SEM) and transmission electron microscopy (TEM) images of the obtained GNPs. The uniform GNP monomers with about 40 nm in diameter were obtained from general reduction in Figure 2(a). By adding a small amount of NaCl into the reaction, a mixed GNPs (GMDT) of monomers (GM), dimers (GD), and trimers (GT) were obtained in Figure 2(b). In this GMDT solution, GD and GT consisting of GNPs 40 nm in diameter are separated by 2 nm in solution with a yield of 43% and 27%, respectively. It is found that the yield of the GD and GT is sensitive to the concentration of NaCl in the reaction mixture. In contrast, when a larger amount (100 and 200 μl) of the NaCl solution was added to the reaction, the yield of GD and GT was much lower than that of the sample shown in Figure 2(b), and larger aggregates could be easily found in the samples (see Figures 2(c) and 2(d)). In order to optimize the yield of GD and GT, one has to optimize the concentration of NaCl in the medium region.

The optical absorbance properties of metal nanostructured materials originate from LSPR, and the spectral position of the LSPR is dependent on the size, shape, and local dielectric environment of the nanoparticle. Therefore, the extinction spectra provide valuable information on the

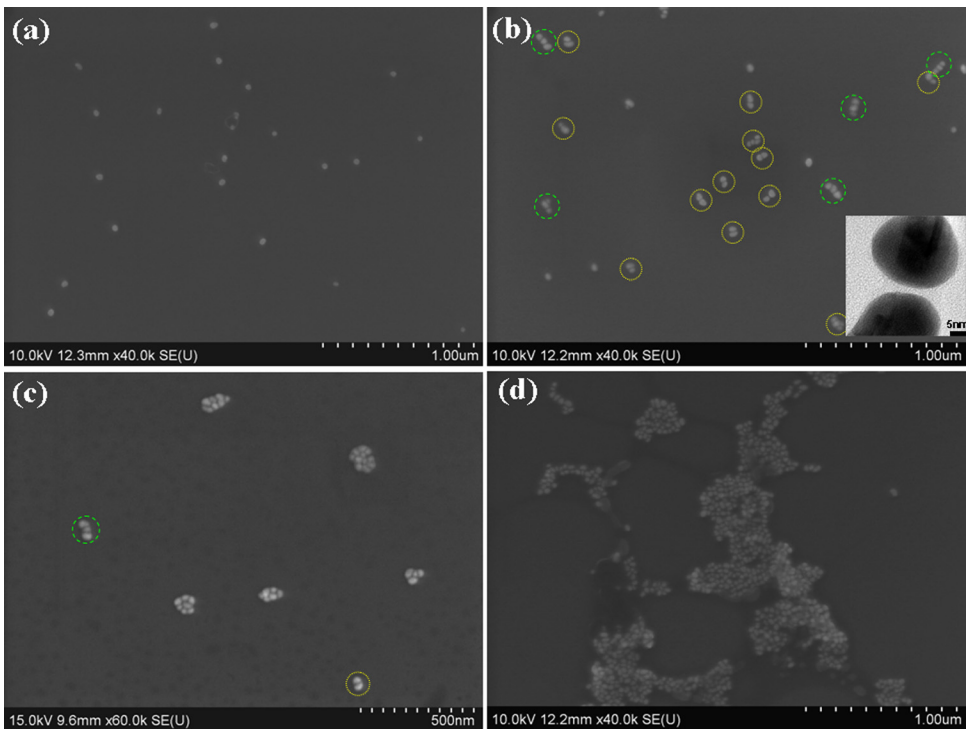

FIG. 2. The SEM images of GNPs prepared with the addition of different amounts of NaCl solution: (a) 0 μl (GM), (b) 50 μl (GMDT), (c) 100 μl and (d) 200 μl. The dimers and trimers are highlighted by yellow and green circles. Inset: the TEM image of the gap.

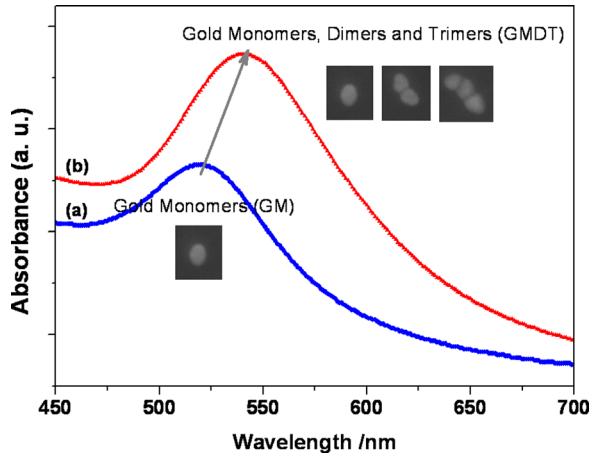

FIG. 3. The absorption spectra of the (a) GM and (b) GMDT. Insets: The SEM images of GM, GD, and GT.

structure of the nanoparticles. Because of the interaction among the aggregated nanoparticles, a red-shift of the LSPR peaks can be found from GD and GT.[24] Figure 3 shows the extinction spectra of GM and GMDT solutions. Compared with GM solution, it was found that a red-shift of the LSPR peak can be observed in the extinction spectrum of GMDT solution. It proves the existence of GD and GT in GMDT solution and also excludes the influence of drying process on preparing the substrates in SEM experiment.

As shown in Figure 4, SEF spectra can be obtained from GMDT and GM solutions with the excitation wavelength of 532 nm. By comparing the peak at 556 nm, it is find that the enhancement factor (E_{SEF}) is about 7 and 5 for GMDT and GM based on the following equation:

$$E_{SEF} = (I_{GNPs} - I_{background})/(I_{reference} - I_{background}), \quad (1)$$

where I_{GNPs} is the fluorescence intensity of Rh6G from GMDT or GM, $I_{reference}$ is the fluorescence intensity from Rh6G, and $I_{background}$ is the background intensity of the spectra. To avoid interference of fluorescence in Raman signal, we use the excitation wavelength at 632.8 nm in SERS

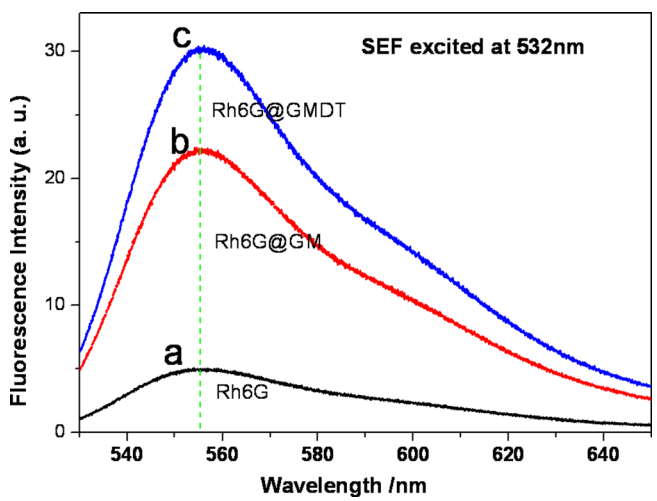

FIG. 4. SEF spectra excited with 532 nm from (a) Rh6G, (b) GM, and (c) GMDT.

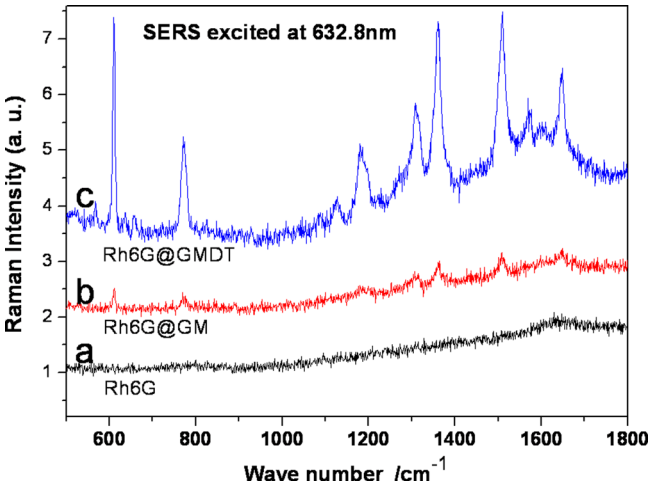

FIG. 5. SERS spectra excited with 632.8 nm from (a) Rh6G, (b) GM, and (c) GMDT.

experiments, in which photon energy is too low to excite Rh6G. From the recorded Raman spectra shown in Figure 5, almost no Raman signal can be found from the only Rh6G solution. In the Rh6G solution containing the GM and GMDT, enhanced Raman signals are clearly observed, and the enhancement of GMDT is much stronger than GM.

By comparing the SEF and SERS spectra in Figures 4 and 5, we can find the following results. First, a clear enhancement of Rh6G on GNPs in SEF and SERS study, and the SERS enhancement factor is much more than SEF; second, the GMDT substrate has a stronger enhancement than GM substrate, especially in SERS spectra; lastly, it is important to note that only fluorescence but no Raman signal could be observed with the excitation wavelength of 532 nm.

To interpret the above experiment results, theoretical simulation with the FEM was done using COMSOL Multiphysics 3.5a (RF Module) software. Optical constants for gold are interpolated from Ref. 27. The incident excitation is described by a plane wave with an instantaneous electric field of the form $E_{inc} = E_0 e^{-i\varphi}$, where $\varphi = \omega t$ is the incident phase and E_0 is the mode profile of the incident light, and the polarization is parallel to the GNPs center line. GNPs in all models are 40 nm in diameter and separated by a gap of 2 nm in the models of GD and GT.

As shown in Figure 6, the simulation results reveal the distribution of the strongest local EM field enhancement is in the gaps of GD and GT, and the enhancement is stronger with the excitation wavelength of 632.8 nm. Since the molecule to be detected could be located anywhere close to the metal surface, the EM field enhancement fact ($|E_{loc}|^2/|E_{inc}|^2$) must be averaged over the entire cluster surface

$$\langle |E_{loc}|^2 / |E_{inc}|^2 \rangle = \frac{1}{\sum_i^j 4\pi R_i^2} \sum_i^j \int_i (|E_{loc}|^2 / |E_{inc}|^2) d\sigma, \quad (2)$$

where R is the radius of the integrated enveloping surface and j is the number of NPs in the simulation cluster. The surface average of $|E_{loc}|^2/|E_{inc}|^2$ response to different distances

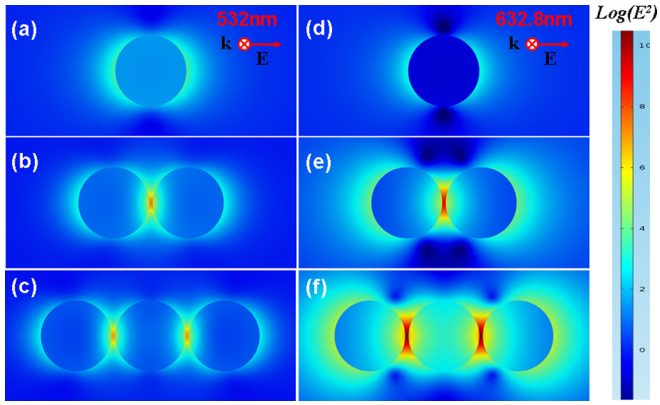

FIG. 6. Images of the simulated distributions of $|E|^2$ were plotted in logarithmic scale with (a)-(c) 532 and (d)-(f) 632.8 nm excitation for GM, GD, and GT.

from GM, GD, and GT can be seen from Figure 7. It is found that the surface average depends on the distance between the NPs surface and the integrated enveloping surface, and the strongest enhancement distance is 1 nm. The stronger enhancement wavelength is at 532 nm for GM but is at 632.8 nm for GD and GT. With the excitation wavelength of 632.8 nm, the GT has a much stronger enhancement than GD.

As shown earlier in the introduction, enhanced local EM field aroused the SEF and SERS effect and that are proportional to $|E_{loc}|^2/|E_{inc}|^2$ and $|E_{loc}|^4/|E_{inc}|^4$, respectively. Since SEF occurs on a certain distance between molecule and GNPs surface, we use $|E_{loc}|^2/|E_{inc}|^2$ of the surface of 2 nm away from GNPs as the SEF enhancement factor. The calculated enhancement factors E_{SEF} and E_{SRES} can be seen in Table I. Because of the relatively low calculated E_{SRES} with 532 nm excitation and the influence of fluorescence signals, the Raman signal cannot be obtained from the SEF spectra in Figure 4. Compare with the E_{SRES} of GM, the GMDT has a much higher enhancement factor with the excitation wavelength of 632.8 nm, which is consistent with the experimental results in Figure 5. The calculated EM enhancement matches well with the results in SERS experiment in GNPs

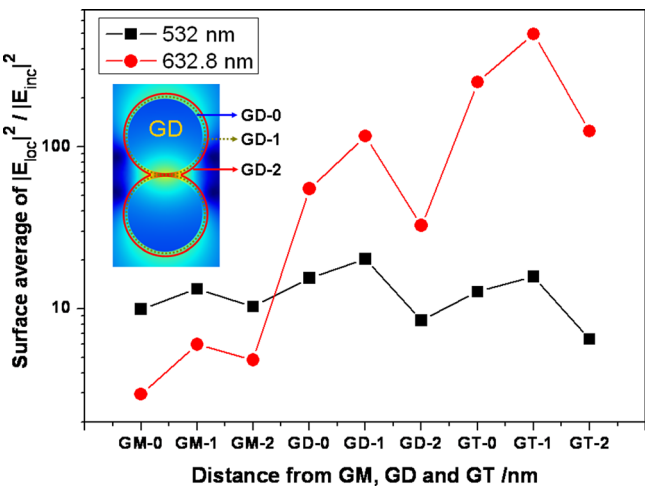

FIG. 7. Surface average of $|E|^2$ with 0, 1, and 2 nm distance from the surfaces of GM, GD, and GT. Inset: Three integrated enveloping surfaces of GD.

TABLE I. The enhancement factor of SEF and SERS excited at 532 and 632.8 nm from GM, GD, GT, and GMDT.

Enhancement Factor	Wavelength/nm	GM	GD	GT	GMDT
E_{SEF}	532	10.3	8.5	6.5	8.5
	632.8	4.8	32.5	125.1	49.2
E_{SERS}	532	175.6	412.1	246.5	296.3
	632.8	36.0	13502.4	246115.2	72267.9

solutions. However, the calculated SEF factor of GMDT is lower than that of GM, which is in contradict to the experimental results shown in Figure 4. Therefore, the experimental results of SEF factor could not be solely explained by the EM enhancement theory and require to include some other effects.

Because SEF mechanism is also related to radiative and nonradiative process, we also investigate the theoretical simulation of radiative and nonradiative processes of fluorescence near GNPs. The molecule is treated as an oscillating classical point dipole, $p(t)$. When a molecular dipole is placed in the vicinity of the metallic nanostructure, its radiative decay rate Γ_0 changes to $\Gamma_{tot} = \Gamma_r + \Gamma_{nr}$. Here, Γ_r represents the energy that reaches the far field, whereas Γ_{nr} accounts for the radiated energy absorbed by the metallic nanostructure owing to material losses. The factor F, defined as $F = \Gamma_r/\Gamma_0$ (Γ_{nr}/Γ_0), represented the radiative (nonradiative) decay rate enhancement, can be given by the ratios of powers inferred from surface integrals over Poynting vector (S), $\Gamma_r/\Gamma_0 = W_r/W_0$, and $\Gamma_{nr}/\Gamma_0 = -W_{nr}/W_0$.[28] The radiated power of the isolated dipole system is $W_0 = \int\int_{\Sigma_0} S_0 \cdot d\Sigma$, where Σ_0 is a closed surface that contain the molecular dipole and S_0 is the Poynting vector in the absence of the GNPs. The radiative and nonradiative powers in the presence of the GNPs are $W_r = \int\int_{\Sigma_r} S_r \cdot d\Sigma$, where Σ_r is a surface that contain the molecular dipole and GNPs, and $W_{nr} = \int\int_{\Sigma_{nr}} S_{nr} \cdot d\Sigma$, where Σ_{nr} encloses only the GNPs. The modified quantum efficiency η is related to η_0 (the quantum efficiency in free space) and the radiative decay rate enhancement F according to

$$\eta = \eta_0/[(1-\eta_0)/F + \eta_0/\eta_{NPs}], \tag{3}$$

where $\eta_{NPs} = \Gamma_r/\Gamma_{tot}$, is the quantum efficiency of the NPs. By considering the EM enhancement of NPs, the modified fluorescence enhancement is written as

$$E = \frac{\eta}{\eta_0} \times \frac{\langle |E_{loc}|^2 \rangle}{\langle |E_{inc}|^2 \rangle}. \tag{4}$$

According to the above equation, the fluorescence enhancement depends on the factor F, the NPs efficiency η_{NPs}, and the initial quantum efficiency η_0. For Rh6G molecule,[29] the calculated fluorescence enhancement factor E, as a whole were 4.8 and 7.5 for GM and GMDT system, respectively. So, combining the enhancements of these two different SEF theories, the experimental results in Figure 4 can be understood.

We note that the calculated enhancement of SEF is a little higher than the experimental E_{SEF} obtained from Figure 4. It was due to the fact that the fluorophores are not just sitting the close vicinity of the GNPs in GMDT solution, and the enhanced regions are only a part of the excitation region. Moreover, the polarization of laser cannot parallel to all the dimers and trimers in GMDT solution. However, the calculated SEF enhancement can present a qualitative analysis for the experimental results. In a word, although the GMDT substrate does not show a much higher intensity enhancement compared to the GM substrate in SEF measurements, it shows a significant enhancement in SERS, which can be seen in both the experiment and simulation results.

IV. CONCLUSIONS

We report a simple wet chemistry method to synthesize dimers and trimers gold nanoparticles based on the boil reaction. The amount of NaCl added to the reaction solution played a critical role in determining the yield of the GD and GT. In such structures, GNPs can come close to each other to create "hot spot" for strong enhancement of the localized EM field. From the SEF and SERS spectra, it is clear that the GMDT has a better enhancement than the GM, which is more obvious for SERS. Using FEM, the enhancement factors of SEF and SERS can be calculated from the EM field intensity distribution. In addition, the enhanced radiative decay rate of fluorescence has to be considered in SEF in order to match with the observed experiment results. We believe that this well-defined GMDT substrate hold great promise for ultrasensitive detection and are expected to find a range of applications in fields such as biological and chemical sensor, photonics, and environmental science.

ACKNOWLEDGMENTS

This work was supported by the National Natural Science Foundation of China (Grants 11174190), the National Basic Research Project of China (Grant 2009CB930700), the Fundamental Research Funds for the Central Universities (No. 2010ZYGX025), and the Innovation Funds of Graduate Programs, SNU (No. 2010CXB004).

[1]M. Moskovits, Rev. Mod. Phys. **57**, 783 (1985).
[2]J. Dong, S. Qu, Z. Zhang, M. Liu, G. Liu, X. Yan, and H. Zheng, J. Appl. Phys. **111**, 093101 (2012).
[3]D. K. Lim, K. S. Jeon, J. H. Hwang, H. Kim, S. Kwon, Y. D. Suh, and J. M. Nam, Nat. Nanotechnol. **6**, 452 (2011).
[4]Y. R. Fang, Y. Z. Li, H. X. Xu, and M. T. Sun, Langmuir **26**, 7737 (2010).
[5]J. F. Li *et al.*, Nature **464**, 392 (2010).
[6]S. Baluschev, F. Yu, T. Miteva, S. Ahl, A. Yasuda, G. Nelles, W. Knoll, and G. Wegner, Nano Lett. **5**, 2482 (2005).
[7]Z. L. Zhang, X. R. Tian, H. R. Zheng, H. X. Xu, and M. T. Sun, Plasmonics "Tip-enhanced Ultrasensitive Stokes and Anti-Stokes Raman Spectroscopy in High Vacuum," (unpublished). doi: 10.1007/s11468-012-9426-5.
[8]M. T. Sun, Z. L. Zhang, H. R. Zheng, and H. X. Xu, Sci. Rep. **2**, 647 (2012).
[9]J. Dong, H. R. Zheng, X. Q. Yan, Y. Sun, and Z. L. Zhang, Appl. Phys. Lett. **100**, 051112 (2012).
[10]M. T. Sun and H. X. Xu, Small **8**, 2777 (2012).
[11]C. D. Geddes and J. R. Lakowicz, J. Fluoresc. **12**(2), 121 (2002).
[12]E. Fort and S. Gresillon, J. Phys. D: Appl. Phys. **41**, 013001 (2008).
[13]M. Fujimaki, K. Awazu, and J. Tominaga, J. Appl. Phys. **100**, 074303 (2006).
[14]J. R. Lombardi and R. L. Birke, J. Chem. Phys. **136**, 144704 (2012).
[15]K. Ray, R. Badugu, and J. R. Lakowicz, Langmuir **22**, 8374 (2006).
[16]N. Akbay, J. R. Lakowicz, and K. Ray, J. Phys. Chem. C **116**, 10766 (2012).
[17]H. X. Xu, E. J. Bjerneld, M. Käll, and L. Börjesson, Phys. Rev. Lett. **83**, 21 (1999).
[18]A. Aftab and G. Reuven, Nano Lett. **12**, 2625 (2012).
[19]H. X. Xu, X. H. Wang, M. P. Persson, H. Q. Xu, M. Käll, and P. Johansson, Phys. Rev. Lett. **93**, 243002 (2004).
[20]H. R. Zheng, L. M. Xu, Z. L. Zhang *et al.*, Sci. China, Ser. G **53**, 10 (2010).
[21]J. Zhang, J. Malicka, I. Gryczynski, and J. R. Lakowicz, J. Phys. Chem. B **109**, 7643 (2005).
[22]L. Guerrini, J. V. Garcia-Ramos, C. Domingo, and S. Sanchez-Cortes, J. Raman Spectrosc. **41**(5), 508 (2010).
[23]Z. L. Zhang, H. R. Zheng, M. C. Liu, H. Zhang, B. Y. Yin, and H. J. Zhang, J. Nanosci. Nanotechnol. **11**, 9803 (2011).
[24]Z. B. Wang, B. S. Luk yanchuk, W. Guo, S. P. Edwardson, D. J. Whitehead, L. Li, Z. Liu, and K. G. Watkins, J. Chem. Phys. **128**, 094705 (2008).
[25]D. Kim, S. Park, J. H. Lee, Y. Y. Jeong, and S. Jon, J. Am. Chem. Soc. **129**, 7661 (2007).
[26]W. Li, P. H. C. Camargo, X. Lu, and Y. Xia, Nano Lett. **9**, 1 (2009).
[27]P. B. Johnson and R. W. Christy, Phys. Rev. B **6**, 4370 (1972).
[28]Y. Xu, R. K. Lee, and A. Yariv, Phys. Rev. A **61**, 033807 (2000).
[29]R. F. Kubin and A. N. Fletcher, J. Lumin. **27**, 455 (1982).